Astronomy & Astrophysics

Evidence of intense hot (≃340 K) dust emission in 3CR radio galaxies

The most dissipative source of cooling in AGNs

B. Rocca-Volmerange[1,2] and M. Remazeilles[1]

[1] Institut d'Astrophysique de Paris, 98bis Bd Arago, 75014 Paris, France
 e-mail: brigitte.rocca@iap.fr
[2] Université de Paris-Sud XI, I.A.S., 91405 Orsay Cedex, France

Abstract. The spectra of the powerful 3CR radio galaxies present a typical distribution in the far-infrared (FIR). From the observed radio to X-ray spectral energy distribution (SED) templates, we propose to subtract the typical energy distributions of, respectively, the elliptical galaxy host and the synchrotron radiation. The resulting SED reveals that the main dust emission is well fitted by the sum of two blackbody components at the respective temperatures 340 K ± 50 K and 40 K ± 16 K. When the AGN is active, the energy rate released by hot dust is much more dissipative than cold dust and stellar emission, even when the elliptical galaxy emission is maximum at the age of ≃90 Myr. Hot dust appears as a huge cooling source which implies an extremely short time-scale t_{cool}, on balance with the short gravitational time-scale t_{grav} of massive galaxies. The dissipative self-gravitational models (Rees & Ostriker 1977) are favoured for radio sources. They justify the existence of massive radio galaxies discovered at $z = 4$ (Rocca-Volmerange et al. 2004). The synchrotron emission is emitted up to the X-ray wavelength range, so that Extreme X-ray Objects (EXO) could be identified with 3CR radio sources. To confirm these results in the infrared, an analysis of larger data samples from ISO and SPITZER is needed.

Key words. galaxies: evolution – infrared: galaxies – galaxies: active – galaxies: formation

1. Introduction

In Rocca-Volmerange et al. (2004), hereafter RV04, we showed that powerful radio sources are hosted by the most massive galaxies. Based on measurements of stellar masses with robust evolution models, the maximum mass is limited by the fragmentation limit at $\simeq 10^{12}$ $M_\odot$ (Rees & Ostriker 1977; Silk 1977) clarifying the interpretation of the so-called $K-z$ relation in the K-band Hubble diagram. Moreover from this diagram interpretation, RV04 puts a constraint on galaxy types: only host galaxies of elliptical type fit the radio galaxy distribution from $z = 0$ to 4. However at $z = 4$, the time-scale of mass accumulation becomes so short that to form massive galaxies requires short dissipative time scales, of the same order as gravitational time scales.

Typical UV to radio SEDs of 3CR galaxies were compiled from observations by ISO, IRAS and IRAM in Andréani et al. (2002). From the FIR emission, they conclude that there is a double emission respectively from a dusty torus and a larger-scale (cooler) dust distribution in the host galaxy. We propose a more detailed analysis of the dust temperatures by a multi-component approach disentangling the star and jet spectral contributions.

Statistically well identified by their high radio power, 3CR galaxies are also hosts of massive stellar populations, which contribute to the optical and infrared emission. In the near-infrared, the stellar emission of the radio sources is often similar to that of the populations of massive elliptical galaxies. In the mid-infrared, the recent analysis of a significant sample of early-type galaxies observed with ISOCAM (Xilouris et al. 2004) shows that the emission is dominated by the presence of the Polycyclic Aromatic Hydrocarbon (PAH) feature at 6.7 μm, an excess of hot dust at 15 μm and a cold thermal component at 30–40 K peaking between 70 and 100 μm. A comparison of the FIR emission of elliptical galaxies with that of radio sources should give a specific information on the AGN contribution. Using templates from the code PÉGASE (www.iap.fr/pegase) we are able to predict the stellar emission at all galaxy ages while the synchrotron radiation contributes to SEDs when the AGN is active.

Another objective is to estimate the cooling time-scale at the earliest phases of galaxy formation. Instead of using the classical cooling function of only helium and hydrogen clouds, each dissipative source (stars, gas, dust and AGN) has to be individually considered during galaxy evolution. In Sect. 2, we compare the various components to the averaged observed SED

of 3CR radio galaxies. Section 3 presents the best fit of dust emission with the sum of two main blackbody laws, of which the hot component is an intense source of dissipation. Section 4 predicts the dissipation rate from various sources (synchrotron, stars, gas and dust) defining a cooling time scale to be compared with the dynamical time scale. The last section gives the discussion and conclusion.

2. Stellar and synchrotron emission

The striking similarity of the radio-to-UV SEDs of 3CR radio galaxies and quasars (see Figs. 1 to 4 in Andréani et al. 2002) indicates that the various components of these complex systems have similar properties. All the spectra present a specific gap from the radio emission for $\lambda < 10^7$ Å (1 mm), presuming similar properties of the dust in 3CR galaxies.

2.1. Stellar and nebular components

Radio galaxies are embedded in massive elliptical galaxies, even at high redshifts (van Breugel et al. 1998; Lacy et al. 2000; Pentericci et al. 2001), of high luminosities $L \simeq 3$ to $7\,L_*$ (Papovich et al. 2001) which may reach $10\,L_*$ (Mc Lure et al. 2004). The 3CR radio galaxies are the most powerful galaxies in the K-band Hubble diagram, they are located at the brightest limit of the galaxy distribution, the so-called $K - z$ sequence. In RV04, we checked with the evolution model PÉGASE that only scenarios for elliptical galaxies of $10^{12}\,M_\odot$ baryonic masses are able to explain the $K - z$ sequence. However very strong emission lines are typical of massive radio galaxies while elliptical galaxies show no emission lines. To confirm our mass estimates, we also included in our modeling the nebular emission of gas ionized by the AGN component (Moy & Rocca-Volmerange 2002), computed with the code CLOUDY (Ferland 1996). In the present paper (Fig. 1), the observed radio galaxies in the Hubble K diagram are well fitted by $10^{12}\,M_\odot$ elliptical models and AGN emission lines. The emission line widths are assumed to be 10 Å at $z = 0$. The redshift of elliptical galaxy formation is $z_{\rm for} = 30$, instead of $z_{\rm for} = 10$ in RV04. Our conclusions on the galaxy formation theory which is characterized by the fragmentation limit of $10^{12}\,M_\odot$ remain unchanged, allowing us to adopt this mass for 3CR powerful radio galaxy hosts.

The NIR predictions from 1 to 5×10^4 Å (1 to 5 μm) are strongly dependent on the modeling of cold star populations. The effective temperatures of giant branch and asymptotic giant branch stars, as well as the mass population density are crucial but are not accurately estimated. We checked with Fig. 2 in Fioc & Rocca-Volmerange (1996) that the PÉGASE elliptical model predicting stellar populations on the two branches is in agreement with the observational template. However we still admit that the separation of the stellar and hot dust component will be less robust from $\lambda = 1$ to 5×10^4 Å than for $\lambda > 5 \times 10^4$ Å.

Most scenarios of galaxy evolution take into account extinction by dust, computed with a transfer model in ellipsoidal or slab geometries (Fioc & Rocca-Volmerange 1997). However in the elliptical scenario, galactic winds expel gas and dust at
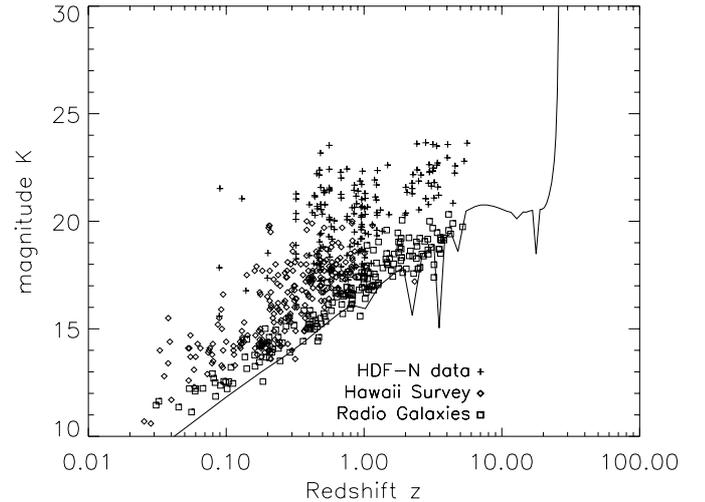

Fig. 1. The distribution of radio (squares) and field (diamonds, crosses) galaxies in the K-band Hubble diagram, compared to the predicted sequence of elliptical galaxies of masses $10^{12}\,M_\odot$; the adopted redshift of formation is $z_{\rm for} = 30$. Sequences with other masses and redshifts of formation were already tested in Rocca-Volmerange et al. (2004). The main emission lines from AGN appearing in the K band for $0 < z < 30$ (H$_\alpha$, [OIII]5007 Å + H$_\beta$, [OII]3727 Å and Ly$_\alpha$1215 Å) are also plotted with a width of 10 Å at $z = 0$. Previous conclusions are unchanged: $10^{12}\,M_\odot$ is the upper mass limit of galaxies and also the fragmentation limit predicted by the models.

1 Gyr, so that at $z = 0$ our modelling only simulates the stellar emission. In the following, we shall adopt the SED model of elliptical galaxies to predict the underlying populations of radio sources.

2.2. Synchrotron radiation

The synchrotron radiation in radio galaxies follows a power law $F_\nu = \nu^\beta$. Observations in the radio domain are well fitted by $\beta = -1.04$ (Andréani et al. 2002).

The energy distribution and intensity of the dust emission can be derived from the radio-to-UV SED template of 3CR radio galaxies: by comparing the stellar and synchrotron emission with the composite spectrum of averaged 3CR galaxy SEDs, we find a large unresolved bump from $\lambda = 1$ to 500×10^4 Å (1 to 500 μm and $\log(\nu_{\rm Hz}) \simeq 12$ to 15). The average redshift $z = 0.5$ of the observational sample has been corrected to the rest frame. The comparison is presented in Fig. 2.

3. Main hot and cold dust components

The various grains found in the interstellar medium (Desert et al. 1990) contribute at different levels to the total FIR emission of radio sources. The global FIR emission is described as the superposition of blackbody (BB) laws depending on the distribution of grain temperature, size and species. We do not consider the emission signatures typical of PAH, generally attributed to star formation: in evolved elliptical galaxies, the star formation activity is nil or very low. The first result of the analysis is that it is not possible to reproduce the IR bump with one single BB temperature. We then propose to limit the
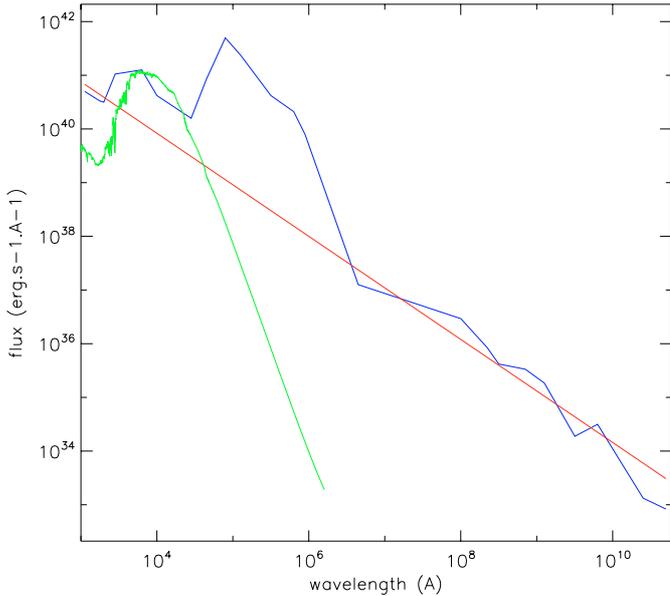
Fig. 2. The observed energy distribution of 3CR galaxies by Andréani et al. (2002) (full blue line) in a large wavelength range ($\lambda = 10^3$ to 10^{10} Å) is plotted with the stellar SED of the 10^{12} $M_\odot$ elliptical template (dotted green line) from PÉGASE and the synchrotron power law (full red line). The synchrotron radiation might contribute to the X-ray emission (see discussions on the so-called *EXO* (Extreme X-ray Objects) below).
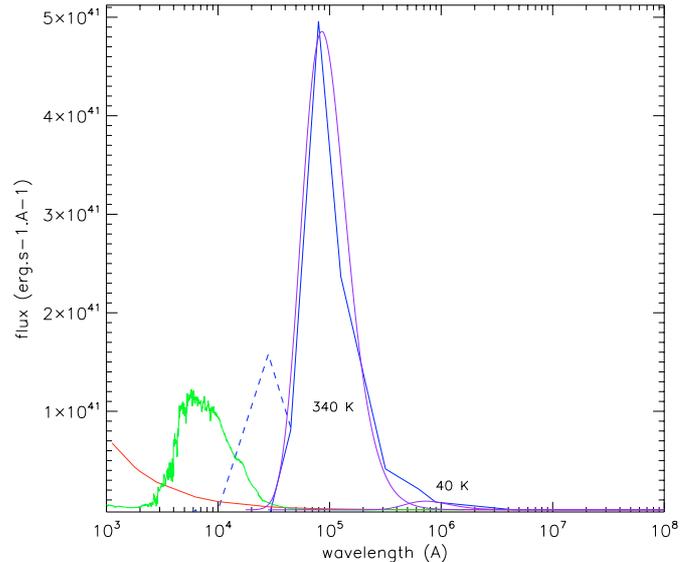

Fig. 3. The three main fluxes contributing to the radiative energy of the 3CR radio galaxy sample are the elliptical SED (green line), the synchrotron power law (red line) and the two blackbody laws (pink lines) of respectively 340 K ± 50 K and 40 K ± 16 K. The dust emission (blue lines) is derived from the observations after subtraction of stellar + synchrotron emissions. For $\lambda > 3 \times 10^4$ Å, the fit with the sum of two blackbody laws is robust (full line), while for $\lambda < 3 \times 10^4$ Å, the peak at the temperature $\simeq$900 K (dashed line) is less accurate.

decomposition to only two BB laws. The second result is the excellent fit for two extreme temperatures: the hot component corresponds to a BB temperature of 340 K ± 50 K, the cold component to a BB temperature of 40 K ± 16 K. Figure 3 presents the stellar and synchrotron fluxes F(λ) as a function of the wavelength λ and a comparison of the two black-body laws with the observed bump. From the Wien law, the 340 K ± 50 K BB emission peaks at the wavelength 8.5 ± 1.25 × 10^4 Å (8.5 ± 1.25 μm). In 3CR radio galaxies, this hot component is an extreme source of energy dissipation. A similar temperature was observed in the far-infrared continua of quasars (Wilkes et al. 1998) but in quasars it is not possible to disentangle the contribution of other components, in particular stellar. Because it is found in radio galaxies, this hot component may be attributed to the active galaxy nucleus (AGN); however, the hot dust component at 260 K found in early-type normal galaxies from ISOCAM data (Ferrari et al. 2002) could be of similar nature, even if its luminosity is much lower.

The wavelength peak for 40 K as derived from the Wien law is at 7.2 × 10^5 Å (72 μm). Fluxes at mid-height correspond to an accuracy of ±16 K. This cold component may be compared with the already known 40 K–60 K temperatures found by the *ISO* and *SPITZER* telescopes in dusty evolved galaxies (Blain et al. 2004; Xilouris et al. 2004).

Qualitatively this result of two components is confirmed by the splendid IRAC/SPITZER image of the nearby radio galaxy Centaurus A (Fazio et al. 2004). A third emission peak at $\simeq 3 \times 10^4$ Å (3 μm) may be present in the data (dashed line in Fig. 3). The disentangling of the cold stellar and very hot ($\simeq$900 K) dust emission is less robust and of minor importance for the energy balance.

4. The balance of energy dissipation rates

The classical cooling function predicted for initial clouds of hydrogen and helium (Rees & Ostriker 1977, and references therein) becomes insufficient, and may be wrong, when intense cooling sources are activated during galaxy formation. While stellar and cold dust emission, in particular in case of rapid metal enrichment, depends on the star formation rate, the cooling processes due to the AGN are dissipative only when the AGN is active. However the cooling processes efficiently contribute to the decrease of the cooling time-scale t_{cool}. We propose to estimate hereafter the radiative energy balance during the star formation evolution when the AGN is active. We integrated all the previously considered fluxes (stellar SEDs, BB laws, power law) over their largest wavelength domain. The dissipative energy rate dE/dt in erg s^{-1} is then computed for all sources. For simplicity, we separate stellar and AGN sources. Stellar sources evolve on the galaxy time-scale ($\simeq$14 Gyr) with passive and active evolution while AGN, supposed to be active at an arbitrary time, have a short lifetime ($<10^8$ years).

– The supernova rate is predicted at all ages from the evolution scenario of elliptical galaxies. If we adopt an average luminosity of $10^{42.5}$ erg s^{-1} from the Nomoto models, the radiative energy rate is a minor component of the global emission. In fact, a major fraction of the explosion energy heats the interstellar medium to escape velocity. For more detailed predictions, neutrinos should be taken into account so our results are a lower limit.

– For the gas ionized by massive stars, hydrogen and oxygen lines are the strongest sources of dissipation through the main lines (Ly1215 Å, Hα, Hβ, [OIII]5007 Å,

[OII]3727 Å). The evolution of the number of ionizing photons, ~70% of the Lyman continuum photons N_{Lyc} is predicted by PÉGASE and the emission lines are those of a classical HII region at the electron temperature of 8000 K. The line intensities are then derived by taking into account the metallicity evolution of the gas.

– Huge envelopes of gas ionized by the AGN are observed at all z in the most powerful radio galaxies, in particular around the most distant ones (van Ojik et al. 1997). Emission lines due to AGN have been computed with the code CLOUDY, assuming solar metallicity, a photo-ionisation parameter log $U = -2$ and a density of $100\,cm^{-3}$.

– The dissipative energy of stellar emission is computed for all ages with the bolometric luminosity as a function of time, a standard output of the code PÉGASE.

– The synchrotron radiation, mainly efficient in active AGNs, contributes only to a fraction of the total radiative energy. The power law is integrated over the whole energy range from X-rays to radio.

– The hot and cold dust components, as found in the previous section, dissipate energies at rates dE/dt, which are derived from the integration of the blackbody laws over their respective wavelength domains.

We plot all the dissipation rates in Fig. 4. We arbitrarily assume an AGN active at 1 Gyr. The hot dust component is luminous when the AGN is active while the cold component, also found in elliptical galaxies, is supposed to follow the evolution of the host galaxy metallicity. As a result, when the AGN is active the most important source of dissipation is the hot dust component at ≃340 K.
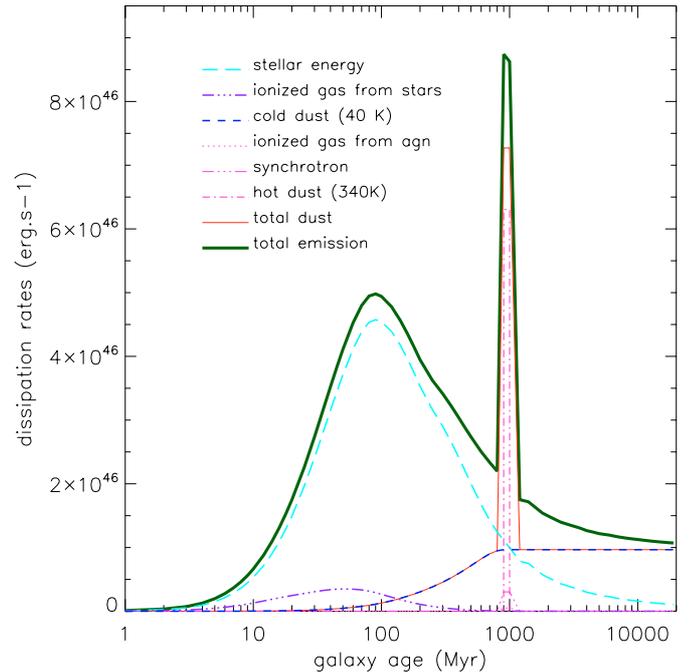

Fig. 4. Various stellar (blue color) dissipative rates dE/dt in erg s^{-1} as a function of time: stellar continuum (dashed light blue line), ionized gas from massive stars (dash-doubled dot violet line), cold dust depending on metals processed by stars (dashed blue line). Dissipative rates due to the AGN formed at 1 Gyr (pink/red color): ionized gas from AGN (dotted clear pink line), synchrotron (dashed-double dot pink line), hot dust (dashed-dot red line). The total dust emission is the pink full line and the sum of all rates is the full green line. The radiative energy from supernova explosions is too faint and has therefore not been plotted; the energy in neutrinos has not been taken into account.

5. Discussion and conclusion

Based on SEDs of 3CR radio galaxies observed from the X-ray to radio domain, we identify the dust emission by subtraction of the template of elliptical galaxies and of the synchrotron power law. Two main components of dust black body (BB) emission (and a possible minor hotter component) are revealed in the $F(\lambda) - \lambda$ diagram, while the classical diagrams $F(\nu) - \lambda$ (or $\nu\,F(\nu) - \lambda$) (Haas et al. 1998) are less suitable for component separation.

The hot dust emission peaks at the wavelength of 8.5 ± 1.5 × 10^4 Å, corresponding to a blackbody temperature of 340 K ± 50 K. This component is in agreement with the standard AGN molecular torus model (Pier & Krolik 1993), embedded in a cooler component. However, if we make a comparison with the IRAC/Spitzer image of Centaurus A (Fazio et al. 2004) we see that the bright hot grain structure is not in the inner core but within a larger structure. Many speculations on the origin of the hot grains are possible, we only conclude that there is a large amount of dust photo-heated by the AGN.

The uncertainty in the hot BB temperature at the maximum includes errors due to calibration and to the modeling of the stellar emission. From Fig. 3, the stellar emission is seen to be negligible at about 8 × 10^4 Å. The large error of ±50 K means that the resolved signatures of PAH observed at respectively 7.7 μm and 8.6 μm (Puget & Leger 1989) could be included in this peak located at ≃8 μm.

The most important uncertainty concerns the total emission at wavelengths around 3 × 10^4 Å. This domain is highly sensitive to the subtraction of the stellar component. Moreover observational data around this wavelength are highly dispersed: a large variation of emission between quasars and radio galaxies is shown by Andréani et al. (2002). At this wavelength, the authors present an extreme value for quasars which would indicate a strong emission peak while for radio galaxies, the peak is significantly weaker energetic.

The main difference with previous studies of active galaxies concerns the star formation. While starburst activity is preferentially investigated in Ultra Luminous Infra Red Galaxies (ULIRG) (Genzel & Cesarsky 2000), star formation is of minor importance in radio sources, which are dominated by the evolved population of elliptical galaxies. However, a puzzling question is arised by the comparison with PAH. A peak of emission centred at the wavelength of 8.5 ± 1.5 × 10^4 Å peak is also found in the ULIRGs (Ultra Luminous Infra Red Galaxies). In general attributed to the PAH, the peak is not thermal and cannot be identified to a black body law but to an instable episodic excitation. It is still premature to decide if there is a link between the 8.5 μm peak discovered in strong ULIRGs and the

8.5 μm peak in powerful radio galaxies. But the similarity of the two peaks deserves further analyses of hidden AGN in starbursts or/and of star formation in AGN environments.

The cool component at 40 K is at about the same temperature as in elliptical galaxies (Xilouris et al. 2004). Thus its origin is not necessarily linked to the presence of the AGN but probably to dusty populations of stars (low-mass AGB stars or others). Moreover, because stellar winds in elliptical galaxies must eject gas and dust, we need to justify the presence of dust. One possibility is that galactic winds expel the interstellar gas, while the denser and more embedded dust component is maintained in the galaxy centre environment. Grains, more massive than gas, could fall into the galactic center more rapidly (or be ejected with less efficiency) than the gaseous component; this process may also depend on the angular momentum. The time scale of grain infall towards the center will then be shorter than the time scale of interstellar gas heating.

Are these results for 3CR radio galaxies acceptable for all AGNs? 3CR radio galaxies are the most powerful and massive galaxies hosting super massive black holes (McLure & Dunlop 2002). If dust emission, in particular by hot dust, is due to a collapsing process of dust towards the centre, the origin of the dust has nothing to do with the presence of an AGN which only heat grains and make them luminous. It might be linked to a star formation process if massive stars are totally embedded in dusty clouds since no evidence of SED signatures due to starbursts is revealed in the optical part of the SED. Whatever the origin of the energetic photons heating the hot dust, the energy released by this dust is considerable. An approximate dynamical time scale $t_{grav} = 1/(G\rho)^{1/2} \simeq 600$ Myr becomes comparable to the cooling time scale during the AGN phase. The total energy dissipated by the 340 K emission, integrated over the AGN life time (10^8 yr) gives a time scale $t_{cool} > 400$ Myr. Our evaluations show that t_{grav} and t_{cool} are quite comparable and the dissipation may regulate the self-gravitational collapse models of galaxy formation (Rees & Ostriker 1977). The dissipation factor may be lower at higher redshifts where metals and dust masses are significantly lower. However, in the case of a massive initial gas reservoir, the collapse is extremely rapid, metal enrichment follows and finally the grain emission is dominant. Another source of uncertainties is the energy released by neutrinos from supernova explosions, so that the presence of an AGN might not be necessary to dissipate energy on a short time scale, comparable to the gravitational time scale. More detailed observations from the ISO archives and the rapidly increasing data set from the satellite SPITZER are required.

References

Andréani, P., Fosbury, R. A. E., van Bemmel, I., & Freudling, W. 2002, A&A, 381, 389

Blain, A., Chapman, S. C., Smail, I., & Ivison, R. 2004 [arXiv:astro-ph/0404438]

Desert, F.-X., Boulanger, F., & Puget, J. L. 1990, A&A, 237, 215

Fazio, G. G., et al. 2004, Proc. Penetrating Bars through Masks of Cosmic Dust, ed. D. Block, I. Puerari, K. C. Freeman, R. Groess, & E. K. Block (Kluwer, Astrophysics and Space Science Library), 319, in press

Ferrari, F., Pastoriza, M. G., Macchetto, F. D., et al. 2002, A&A, 389, 355

Ferland, G. J. 1996, HAZY, a brief introduction to CLOUDY, Univ. of Kentucky, Department of Physics and Astroniomy Internal report

Fioc, M., & Rocca-Volmerange, B. 1996, in from stars to galaxies, ed. C. Leitherer, U. Fritze-von Alvensleben, & J. Huchra, ASP Conf. Ser., 98, 68

Fioc, M., & Rocca-Volmerange, B. 1997, A&A, 326, 950

Genzel, R., & Cesarsky, C. J. 2000, ARA&A, 38, 761

Haas, M., Müller, S. A. H., Chini, R., et al. 2000, A&A, 354, 453

Lacy, M., Bunker, A. J., & Ridgway, S. E. 2000, AJ, 120, 68

McLure, R. J., & Dunlop, J. 2002, MNRAS, 331, 795

Moy, E., & Rocca-Volmerange, B. 2002, A&A, 383, 46

Papovich, C., Dickinson, M., & Ferguson, H. 2001, ApJ, 559, 620

Pentericci, L., McCarthy, P., Röttgering, H., et al. 2001, ApJS, 135, 63

Pier, E. A., & Krolick, J. H. 1993, ApJ, 418, 613

Puget, J. L., & Leger, A. 1989, ARA&A, 27, 161

Rees, M., & Ostriker, J. 1977, MNRAS, 179, 541

Rocca-Volmerange, B., Le Borgne, D., De Breuck., C., Fioc, M., & Moy, E. 2004, A&A, 415, 931

Silk, J. 1977, ApJ, 214, 152

van Breugel, W., Stanford, S., Spinrad, H., et al. 1998, ApJ, 502, 614

van Ojik, R., Roettgering, H. J. A., Miley, G. K., & Hunstead, R. W. 1997, A&A, 317, 358

Wilkes, B. J., Hooper, E. J., McLeod, K. K., et al. 1998, in The Universe as Seen by ISO, ed. P. Cox, & M. F. Kessler, ESA-SP, 427, 845

Xilouris, E. M., Madden, S. C., Galliano, F., Vigroux, L., & Sauvage, M. 2004, A&A, 416, 41